A R C H I V E S O F M E T A L L U R G Y A N D M A T E R I A L S
Volume 60 2015 Issue 4
DOI: 10.1515/amm-2015-0464

J. JOWSA*#, M. BIELNICKI*, A. CWUDZIŃSKI*

NUMERICAL MODELLING OF METAL/FLUX INTERFACE IN A CONTINUOUS CASTING MOULD

MODELOWANIE NUMERYCZNE POWIERZCHNI MIĘDZYFAZOWEJ METAL/CIEKŁY ŻUŻEL W KRYSTALIZATORZE DO CIĄGŁEGO ODLEWANIA STALI

The behaviour of liquid slag in the mould is one of the key research areas of the continuous steel casting process. Numerical simulations of steel casting in the mould equipped with submerged entry nozzle, intended for slab casting, have been carried out within the study. For modelling the behaviour of the interfaces of the liquid steel – liquid slag – air system, the VOF method was employed. In the conducted simulations, seven different procedures for the discretization of the interface of individual phases were tested. The computation results have revealed that the "entrapment" of fine slag portions into liquid steel occurs in the system under investigation; the cause of this phenomenon is explicated by the Kelvin-Helmholtz theory.

Keywords: continuous casting, numerical simulation, Volume of Fluid method, interface tracking schemes, mould flux entrainment.

Badania zachowania się ciekłego żużla w krystalizatorze mają istotne znaczenie dla procesu ciągłego odlewania stali. W pracy przeprowadzono symulacje numeryczne odlewania stali w krystalizatorze z wylewem zanurzeniowym, przeznaczonym do odlewania wlewków płaskich. Do modelowania zachowania się granic międzyfazowych układu: ciekła stal – ciekły żużel – powietrze zastosowano metodę Volume of Fluid (VOF). Podczas prowadzonych symulacji weryfikowano siedem różnych procedur dla dyskretyzacji granicy rozdziału poszczególnych faz. Wyniki obliczeń wykazały, że w badanym układzie dochodzi do „zaciągania" drobnych porcji żużla do ciekłej stali, przyczynę tego zjawiska tłumaczy teoria Kelvina-Helmholtza.

1. Introduction

In the continuous slab casting process, mould powder is used, which is applied on the surface of liquid steel contained in the mould. Part of this mould powder melts to form a slag layer floating on the steel surface. The forming slag performs a number of important functions, e.g. it protects the steel against oxidation from the air atmosphere, reduces heat dissipation to the atmosphere, assimilates part of non-metallic inclusions and, first and foremost, enables the lubrication of the slab being in contact with the mould walls. The slab movement and the oscillating motions of the mould cause the consumption of the mould powder, which necessitates its continuous addition during the course of the steel casting process.

The shape of the liquid slag–liquid steel interface surface depends on many factors, including the geometry of the mould and the submerged entry nozzle (SEN), steel flow rate, mould powder layer thickness, the physicochemical properties of liquid slag and steel (eg. viscosity, surface tension), and the amplitude and frequency of oscillating motions. The dynamic conditions of liquid slag–liquid steel interface surface formation in the mould determine whether the slag layer correctly performs it main functions, or not. On the basis of numerous experiments and observations, researchers have proposed a number of different hypotheses on the causes of the entrapment of slag into the steel. Larger or smaller slag drops that pass into the steel are one of the causes of internal defects of steel slabs continuous casted. Based on the assessment of various research results, many mechanisms are distinguished, which constitute the cause of slag entrapment into the steel. The most important ones include [1÷3]:

1. meniscus level fluctuations,
2. meniscus freezing and hook formation,
3. argon bubble interactions,
4. slag crawling,
5. von Karman vortex formation,
6. meniscus standing wave instability
7. shear layer instability (Kelvin – Helmholtz instability)
8. upward flow impinging on meniscus
9. meniscus balding.

The research of the formation of the slag and steel interface surface in the mould devoted in recent years a lot of attention. In general, these research activities can be divided into three categories: laboratory tests on water–oil models, industrial tests, and numerical simulations using advanced

* CZESTOCHOWA UNIVERSITY OF TECHNOLOGY, DEPARTMENT OF METALS EXTRACTION AND RECIRCULATION, FACULTY OF PRODUCTION ENGINEERING AND MATERIALS TECHNOLOGY, 19 ARMII KRAJOWEJ AV., 42-201 CZESTOCHOWA, POLAND

Corresponding author: jowsa@wip.pcz.pl

mathematical models. As the direct examination of the behaviour of the slag–steel interface surface in the industrial mould are severely restricted due to conditions prevailing there (high temperature, no transparency of phases), great research emphasis has been placed on modelling with the use of water and silicone oils. Such studies yield, as a result, the representation of the shape of the interface surface and its stability or lack of stability [4], depending on the viscosity and prevailing interfacial stresses [5], as well as steel casting conditions, e.g. flow rate, the immersion depth of the pouring tube and its shape [6]. The studies have confirmed the effect of oil layer thickness and the amplitude of the wave produced in the fluid on the instability of interface behaviour; also, the cause of the formation of von Karman vortices has been established [3]. Studies that substitute steel with water and liquid slag with various oils during simulation of steel casting in the industrial mould have the drawback of failing to fully meet the criteria of similarity, as expressed with the following criterial numbers: Reynolds Number (Re), Froude Number (Fo), Weber Number (We) and Capillar Number (Ca). Therefore, in recent years, with the increase in the computing power of computers and the development of new numerical procedures, computer simulations of the casting of steel are increasingly often carried out [7]. For this purpose, various mathematical models are created, which rely mainly on the solution of the equations of fluid motion (such as the Navier-Stokes equation, the equation of continuity, the equations of turbulence) for single-phase or multiphase systems. For the examination of the behaviour of non-metallic inclusions in the liquid steel present in the mould, Eularian-Lagrangian [8,9] type two phase models are used. To describe the interaction of two immiscible phases in the mould, i.e. gas bubbles and steel, Eulerian-Eulerian [10] type models are used, while for the interaction between slag and metal, the Volume of Fluid (VOF) [11÷13,14] model is most commonly employed. This model implemented in many commercial programs, such as ANSYS Fluent, ANSYS CFX, STAR CCM+ and in a FREE OPEN source type program called Open FOAM.

The quality of representation of the interface in the VOF model depends heavily on factors, such as viscosity, the density and topology of the computation grid (mesh), as well as the employed procedures for the spatial discretization of the variable „volume fraction”. Many publications, where the VOF model is used for simulation of steel and slag behaviour in the mould, do not specify the type of numerical procedure used [11÷13]. The choice of the numerical procedure to discretize the interfacial surface may significantly influence the computation results and distort the interface, or not disclose the important mechanisms of phase interactions.

In order to explain in detail the significance of this influence, appropriately performed numerical studies were undertaken on the facility used for slab casting, equipped with a mould with an immersed symmetrical double-opening ceramic submerged entry nozzle (SEN).

2. Geometrical and operational conditions

The examination of the formation of the layer of liquid slag on the steel surface in the mould equipped with a submerged entry nozzle is described on the example of the casting of 0.220×1.0 m cross-section slab. The immersion depth of the submerged entry nozzle (SEN) used at the plant is 225 mm (measured from the meniscus level to lower edge of the SEN). Submerged entry nozzle has two lateral discharge ports inclined downwards at an angle of 15° in relation to the SEN cross-section. The SEN ports have the shape of 65×120 mm rectangular with rounded corners (a rounding radius of 32.5 mm. The casting speed at the plant for this slab size is 1.3 m/min (equivalent to 2.005 ton of steel/min). Figure 1 shows a mid-mould section together with the immersible SEN (the facility of symmetrical).

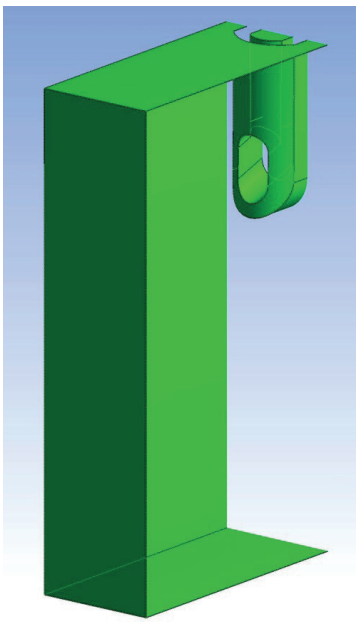

Fig. 1. Schematic viev of the test object – mould equipped with SEN

Numerical simulations were conducted for the unsteady conditions of the casting process. It is assumed that at the initial moment (t = 0) the mould is filled up to the preset height with liquid steel which is covered with a uniform 20 mm-thick layer of liquid slag. At the time t = 0, the steel is motionless ($u_x = u_y = u_z = 0$ m/s). After the time t = 0, the steel flows out through the immersible pouring tube to the mould at the constant flowrate resulting from the adopted slab casting speed. Computations for this flow conditions were conducted for several dozen seconds until the steel motion in the mould had stabilized; the steel velocity field was controlled.

For the purpose of the numerical simulations, the following properties of steel, slag and air were assumed, which are summarized in Table 1

TABLE 1

Properties of liquid steel, slag and air

Properties/ material	Steel	Slag	Air	Unit
Density (ρ)	7010	2600	1.225	kg/m^3
Viscosity (μ)	0.007	0.4	1.789e^{-5}	kg/m·s
Surface tension (σ)	slag/steel	1.6		N/m
	steel/air	0.07		
	slag/air	0.07		

3. Model description

The VOF [15,16] model belongs to the Eularian type category and can be used for systems composed of two or more phase in the number of (k), e.g. for the flows of air bubbles, liquid drops and fluids with a movable free surface. In this model, particular phases are, in terms of computation, regarded as a homogeneous mixture contained within computational cells. Therefore, the mass, momentum and energy transfer equations are solved for a single phase – the mixture, but considering the correct properties of the mixture, e.g. density and viscosity, as defined with the following formula [15]:

$$\rho_{mix} = \alpha_1\rho_1 + (1-\alpha_2)\rho_2 \tag{1}$$

$$\mu_{mix} = \alpha_1\mu_1 + (1-\alpha_2)\mu_2 \tag{2}$$

where $\alpha_1 + \alpha_2 = 1$.
To compute the volume fractions of individual phases (α_1, α_2) for each computational cell, which will be used for the location of the interface surface between successive phases, (k-1) continuity equations are solved [15]:

$$\frac{\partial\alpha_k}{\partial t} = u_k\nabla\alpha_k = 0 \tag{3}$$

It should be noted that the knowledge of local values (α_k) is not sufficient for the definite identification of the interface surface shape, because several different interface surface configurations may correspond to the same value of the volume fraction (α_k), as illustrated in Figure 2.

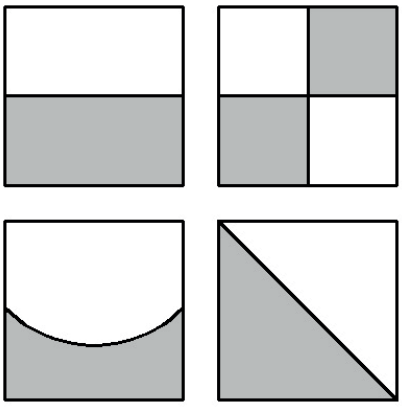

Fig. 2. Possible interface configuration for the same volume fraction (α_k) in the control volume [16]

The direction of the exact run of the interface surface is obtained by special methods. These methods should avoid numerical difficulties due to the discretization of Equation (3), and concerning chiefly the maintaining of a constant interface width (elimination of artificial diffusion) and ensuring the monotonic variation of the variable (α_k). These methods can be generally categorized into geometrical reconstruction interface methods, and methods that use different higher-order discretization schemes, and some of them use also combinations of the first order upwind (UDS) and first order downwind (DDS) schemes.

The first group includes the Donor - Acceptor Scheme (DAS) [15] method and the Simple Line Interface Calculation (SLIC) [17] and Picewise Linear Interface Calculation (PLIC) methods [18]. Included in the second group are the Compressive Interface Capturing Scheme for Arbitrary Meshes (CICSAM) [19] and High Resolution Interface Capturing (HRIC) [20] methods. Methods relying on the geometrical reconstruction of the interface are much more difficult to implement in the case of unstructured or 3D grids and may only be solved in the explicit mode.

Commercial programs, such as ANSYS Fluent, offer several methods for the spatial discretization of Eq. (3), which can be chosen by the user, depending on the time variable discretization method (the explicit and implicit methods).

Within the undertaken studies, a decision was made to verify the adequacy of each of the methods for simulation of the action of flowing steel on the layer of liquid steel floating on the free surface of steel in the mould. Table 2 summarizes a combination of spatial and time discretization methods used in the author's studies.

TABLE 2
The spatial and temporal discretization method

No.	The interface tracking scheme	The discretization scheme
1	First-Order Upwind	Implicit
2	Second-Order Upwind	Implicit
3	Compressive	Implicit Explicit
4	Modified HRIC	Implicit Explicit
5	CICSAM	Explicit
6	Geo-Reconstruct	Explicit
7	Geo-Reconstruct + Level Set	Explicit

The program ANSYS Fluent ver.15 offers the most advanced interface tracking method Coupled Level Set with the VOF model (item no. 7 in Table 2) which uses a combined method of determining the interface by making use of the possibility of exact surface mapping by the Level Set method [21].

The interface between the two fluids is captured by advecting the Level Set function ϕ with the flow velocity **u** [21]:

$$\frac{\partial\phi}{\partial t} = \mathbf{u}\nabla\phi = 0 \tag{4}$$

where ϕ defined as a signed distance from the interface.

The Level Set function is, such that [21]:

$$\phi \begin{cases} < 0 & \text{in fluid 1} \\ = 0 & \text{on the intrface} \\ > 0 & \text{in fluid 2} \end{cases} \tag{5}$$

Because the ϕ function is smooth and continuous, its spatial gradients can be accurate estimates at interface curvature.

Figure 3 illustrates graphically the difference between the VOF method and the Level Set method in the determination of the interface between two fluid phases in a 2D system.

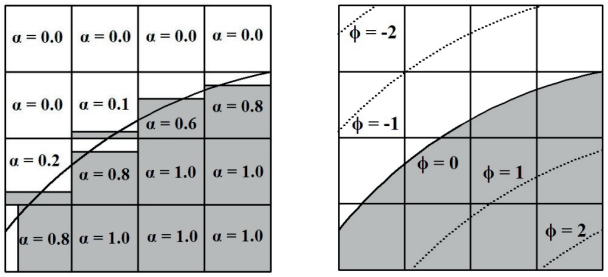

Fig 3. Comparison interface calculation VOF method (with SLIC procedure) – (a) and Level Set method – (b) [22]

In the mathematical model used for numerical simulation of the motion of the phases: the liquid phase and the slag in contact with air, in addition to viscosity forces, also interfacial tension forces must be considered. The importance of interfacial tension forces is defined by the values of the numbers [23]:

$$Ca = \frac{\mu u}{\sigma} \quad \text{dla} \quad Re = \frac{\rho L u}{\mu} << 1 \tag{6}$$

$$We = \frac{\rho L u^2}{\sigma} \quad \text{dla} \quad Re = \frac{\rho L u}{\mu} >> 1 \tag{7}$$

Only in the case, where Ca >> 1 or We >> 1, may the contribution of surface tension forces be omitted in computation. In the case under consideration, it should be expected that the interfacial tension forces can influence the formation of the interface in the steel–slag–air system.

In ANSYS Fluent the continuum surface force (CSF) model proposed by Bracbill [24] and Unwerdi [25] has been implemented such that the addition of surface tension in a source term in the momentum equation is used. In formulation of CSF the surface curvature is computed from local gradients of the volume fraction (α) in surface normal at the interface:

$$\mathbf{n} = \nabla\alpha \tag{8}$$

The curvature of interface (κ) may therefore be expressed in terms of the divergence of the unit normal vector to interface, as follows

$$\kappa = -\nabla \cdot \left(\frac{\nabla\alpha}{|\nabla\alpha|} \right) \tag{9}$$

The surface tension force can be written in terms of the pressure jump across the surface in the whole flow domain to give the CSF formulation for F_σ

$$F_\sigma = \nabla P = -\sigma \left(\nabla \cdot \left(\frac{\nabla\alpha}{|\nabla\alpha|} \right) \right) (\nabla\alpha) \tag{10}$$

where σ - surface tension coefficient, ∇P - gradient of pressure.

4. Computational method details

As the quality of numerical solutions (especially when this applies to the clear and sharp mapping of the interface) is strongly dependent on the quality and density of the computation grid, it was decided that in the zone of the interaction of three phases the length of the computation cell side would be equal to 1 mm.

The mesh generation methods are: structured, unstructured and hybrid. The division between structural and unstructured meshes usually extends to the shape of the elements: two dimensional (2D) structured meshes typically use quadrilaterals, while unstructured meshes use triangles, in three dimensions (3D) the analogous element shapes are hexahedra and tetrahedral.

Based on literature data, a structural grid was chosen in the three phases interaction zone. If the computation grid for the object under examination had been densified only in the phases interaction region and strongly rarefied in the remaining regions (while having made use of the symmetricity of the object), then the number of computation cells would have exceeded 12 million, all the same. The consequence of this would have been too long a computation time, not allowing such simulations to be conducted in real conditions. Therefore, a decision was made to cut out a part of a width of ΔY = 4mm from the center of the object, while imposing the symmetry condition on the cut-out walls. After this operation, the number of computation cells for the examined object is 219 619, which already guarantees that many numerical simulations can be carried out.

Figure 4 shows a view of the computation grid in the X-Z plane being the section of the computational domain of the examined mould; the shaded region is foreseen for the contact of three phases, where the grid side distances equal 1 mm.

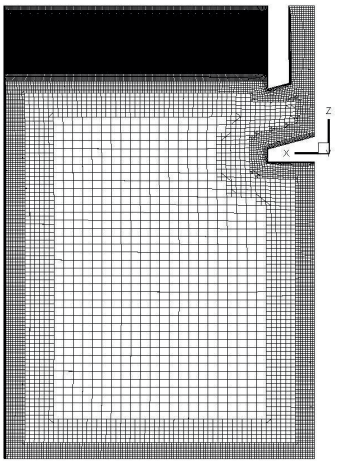

Fig. 4. A view of the computational grid in the X-Z plane being the section of the computational domain of the mould under examination

The ANSYS Fluent program was employed for the computation. In all simulations the PISO scheme was used for the velocity- pressure coupling, and the PRESTO! scheme for the pressure interpolation. For the discretization of the convection term in Eq. (3) or (4), one of the seven methods shown in Table 2 was used. In non-stationary computation for the IMPLICIT scheme, a time step of $\Delta t = 0.001$s was used, while in computation according to the EXPLICIT scheme variable time steps are controlled through the Courant number (Co) defined a follows [23]:

$$Co = \frac{u_{fluid}\Delta t}{\Delta x} \tag{11}$$

where Δx – is the internal length of cell.

For transient VOF calculations under ANSYS Fluent the default value Courant Number is 0.25. The k-ε Realizable turbulence model with Standard Wall Functions is used to capture the flow turbulence. Inlet condition was: turbulent kinetic energy – 0.008723 m^2/s^2, turbulent dissipation rate – 0.02089 m^2/s^3 and mass flow rate of steel – 1.109 kg/s.

5. Numerical results

Numerical simulations were conducted in such a manner that at each time step, convergence to the level of the required residues was achieved. The computation was ended upon finding that the system had attained a steady state – the field of velocity vectors did not change. Figure 5 represents streamlines on the examined object's section after the time of 55s.

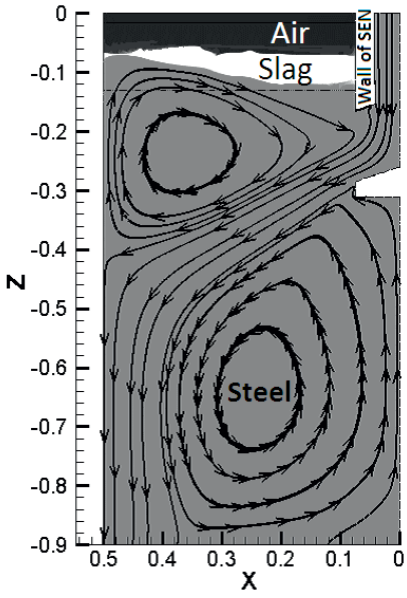

Fig. 5. Streamlines of molten steel obtain from the calculation VOF model

Making use of the computed values of steel velocity in the steel and slag contact zone, the values of the criterial numbers were computed. The velocity values change along the interface surface and across the mould width in the range from 0.05 to 0.2 m/s. Assuming the velocity value equal to u = 0.1 m/s and defining the characteristic dimension as $L=\sqrt{(0.5\times0.004)}$ = 0.044 m, the calculated average Re number value is Re = 4.47. In contrast, the cell Reynolds number value computed with the ANSYS Fluent program is ≈ 3. The obtained results indicate the laminar pattern of flow near the contact between the both phases, that is the steel and the slag. This implies the prevalence of Capillar Number (Ca) over Weber Number (We) for the assessment of the stability of the liquid steel – liquid slag interface. The computed values of the both criterial numbers are $Ca = 4.375e^{-4}$ and We = 1.9. To sum up, it can be noted that the values of the Re, Ca and We numbers show that phenomena determined by the magnitude of interfacial tension forces may significantly change the behaviour of interface surface formation in the system molten steel – air.

When examining the effect of the type of numerical interface discretization procedures (Table 2), the formation of interfaces on the examined object's section was observed within the entire period of time, from the moment of starting filling the mould with steel until the stabilization of steel and slag motion. Figure 6 shows the direct region of liquid slag interaction with the surface of steel in the mould after several dozens seconds of process duration, as computed using selected numerical procedures. Only for the First-Order Upwind (Implicit) procedure no diagram is provided, because the liquid slag phase vanished after approx. 60 s, and the process of reducing the amount of slag started already after 10 s of the steel casting process. On this basis it can be stated that the First-Order Upwind (Implicit) procedure did not prove itself completely.

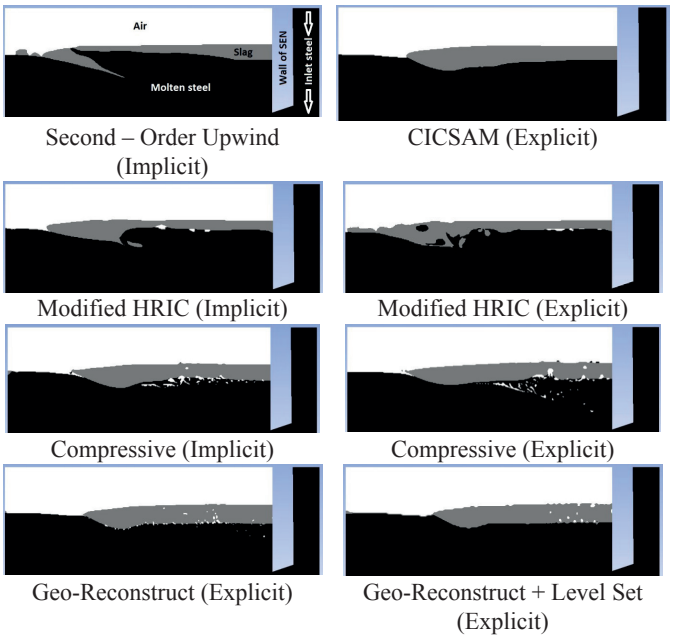

Fig. 6. Phase distribution for the stabilized flow conditions of steel for different numerical methods

In case of the Second-Order Upwind (Implicit) procedure and the remaining procedures, the vanishing of liquid slag was no longer observed; however, the pattern of interface formation for the Second-Order Upwind (Implicit) procedure shows a little probable shape – as very strong interface instability occurs, which manifests itself in the formation of an excessive large slag phase entrapment region, leading to global destruction. This pattern also considerably differs from the remaining patterns shown in Figure 6.

For all examined cases of using different numerical procedures, animation movies were recorded, which depict in detail the behaviour of liquid steel originating from the molten mould powder (the frames were recorded with a step of $\Delta t = 0.05$ s). It is noticed from the movies that the CICSAM (Explicit) is the only method that does not exhibit the entrapment of slag into the steel. For the remaining methods (shown in Figure 6), the formation of gas bubbles and their movement along the steel – slag interface and their partial passing into steel bath, followed by their floating up to the gas phase, also from the slag phase, is also observed. It has been found that when using the Modified HRIC (Implicit) and the Modified HRIC (Explicit) methods, the entrapped slag drops are much larger compared to other methods, ranging from 5 to 8 mm (as measured on the cross-section of a drop, often being irregular in shape). The smallest size of entrapped slag drops is exhibited by the Geo-Reconstruct (Explicit) and the Geo-Reconstruct + Level Set (Explicit) methods.

The numerical simulations were so programmed as to enable also the observation (monitoring) of the dynamic change of the air–slag and slag–steel interface surfaces at selected characteristic points. To illustrate this process, two points of the coordinates X = -0.15 m, Y = 0.002 m and X = -0.45 m, Y = 0.002 m are chosen in the publication. In the obtained diagrams (Figs. 7 and 8), the change in the coordinate corresponding to the movement of the air–slag and slag–steel interfaces is represented.

The variation of the position of the interfaces in Figures 7 and 8 starts at the time t = 0 s (time indicating the start of the simulation); and that time, the thickness of the slag layer at both monitored points was 20 mm. For this presentation, simulations results were chosen using two numerical procedures, namely CICSAM (Explicit) – Fig.7, and Geo-Reconstruct (Explicit) – Fig.8. It should be noted that with the CICSAM (Explicit) procedure, no slag drop entrapment into the steel occurs, while with the Geo-Reconstruct (Explicit) procedure, slag drops get entrapped into the steel, and in addition air bubbles form, which also move within the space of the examined system. In these figures, the horizontal broken lines define the initial position of the interfaces. From Figure 7 it can be seen that after about 20 seconds the movement of the interface stabilizes at the point with the following coordinates: X = -0.45 m, Y = 0.002 m, that is the one situated at the distance of 0.05 m from the narrower mould wall. The thickness of the slag layer after attaining the flow stabilization is approx. 1 mm. By contrast, for the point with the coordinates x = -0.15 m, y = 0.002 m, that is situated near SEN, there occur very small changes in the interfaces between individual phases, and the slag layer thickness is around 23 mm. Simulations using the Geo-Reconstruct (Explicit) method (Fig. 8), exhibit greater variability of the monitored surfaces at the point with the coordinates X = -0.15 m, Y = 0.002 m. This us due to two facts: the first is the detachment of slag particles and their passing into the steel bath, and the second – formation of gas bubbles which then flow along variable paths through the slag–steel interface and get to the air atmosphere. These processes start after a time period of approx. 10 seconds. The thickness of the slag layer at the point with the coordinates X = - 0.45 m, Y = 0.002 m is very small, not exceeding a value of 1 mm.

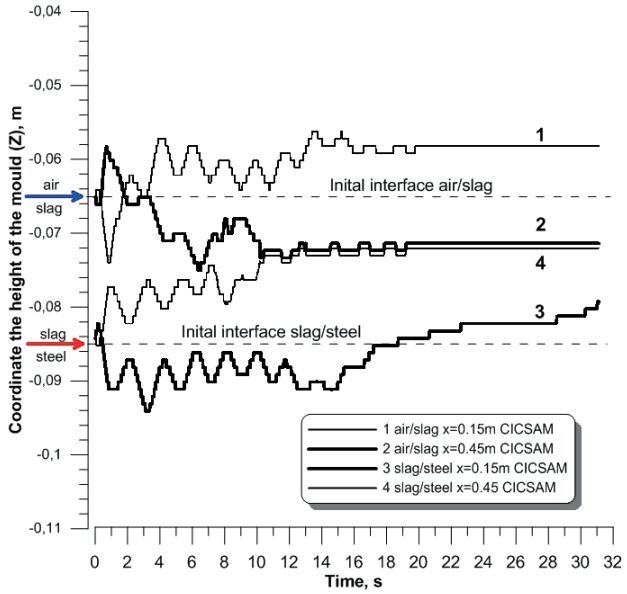

Fig. 7. Change in the position of the air–slag and slag–steel interfaces at two points of the examined system (the CICSAM - Explicit method)

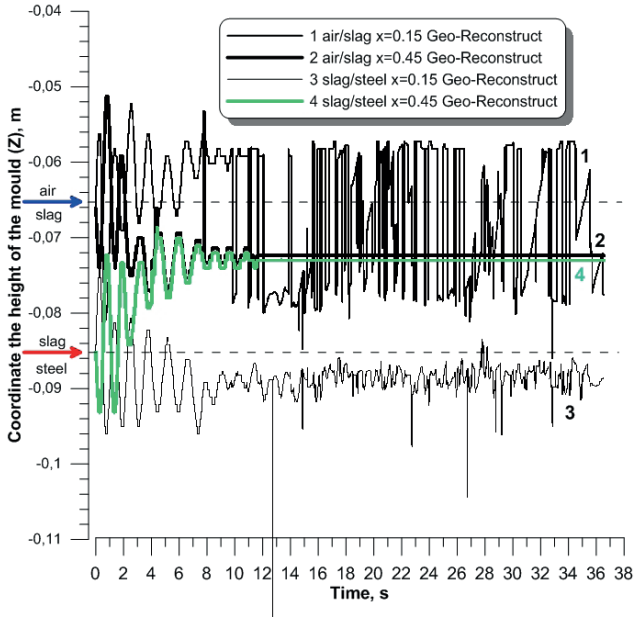

Fig. 8. Change in the position of the air–slag and slag–steel interfaces at two points of the examined system (the Geo-Reconstruct - Explicit method)

To distinguish the details of the processes discussed, an enlarged fragment of the examined system is shown in Figure 9.

It is seen from this figure that in molten steel there are both slag drops (ranging from 1 mm to 2 mm in size) and gas bubbles surrounded by a slag membrane. One can also be notice scarce and very fine steel drops passing into the slag layer (this is particularly visible when observing the picture in three colours – each of them being ascribed to one phase).

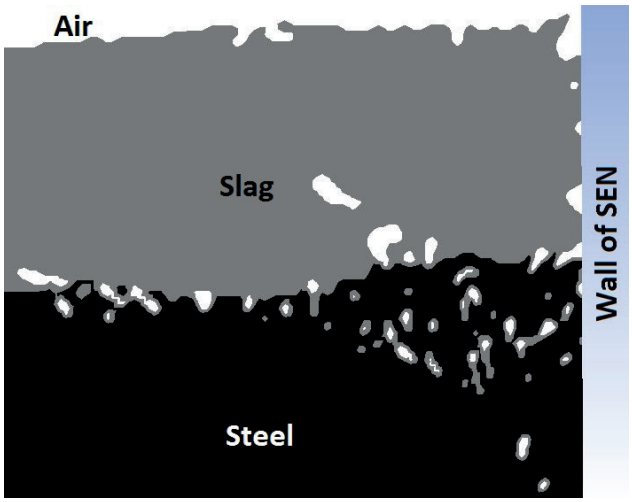

Fig. 9. Entrapment of slag drops and air bubbles into steel according to the Geo-Reconstruct (Explicite) method

6. Discussion

To sum up, it can be concluded form the studies carried out that all of the employed numerical procedures, except for First-Order Upwind (Implicit) and Second-Order Upwind (Implicit), show a similar formation of the layer of liquid slag floating on the steel surface contained in the immersible pouring tube mould used for casting slabs. With the exception of one procedure, all numerical procedures indicate that a liquid slag is entrapped into the steel, with the occurring differences concerning only the amount of entrapped slag and the drop size. The cause of slag entrapment can be seen in the low stability of shearing stresses occurring at the interface. This mechanism is explained in detail by the Kelvin - Helmholtz theory [2]. For explaining this phenomenon, studies on water models with the addition of different silicone oils. Study [2] presents diagrams (Fig. 10) representing the Authors' ideas of the form of the slag–steel system interface.

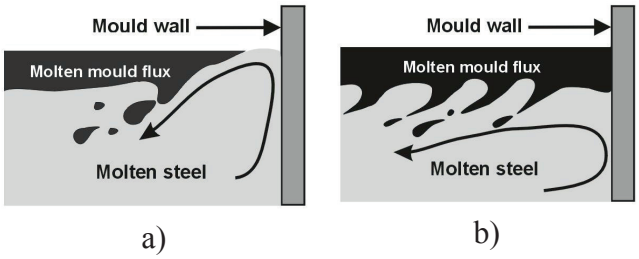

Fig. 10. Illustration of the slag entrapment phenomenon for two cases: with partially exposed steel surface (stationary conditions) – (a) and with no exposed metal surface (non-stationary conditions) – (b) [2]

The view image in Fig. 10a is very similar to the results of simulations using the Modified HRIC (Implicit) procedure, while the view image in Fig. 10b is not in any case similar to the numerical computation results. Based on their laboratory investigations, the authors of work [2] made an attempt to relate the thickness of the silicon oil layer with the amplitude of the wave induced by the water flow, while allowing for the fluid densities and the interfacial tension magnitude, with the aim of determining the critical conditions, where the slag entrapment process occurs. The obtained results were not very satisfactory, so those authors proposed that further studies on this subject should be carried out. Papers [26, 27] present interesting laboratory investigations into the stability of shearing stresses in the water–oil system. The tests were conducted on a test stand including a drive, roller and camera. They were found a relationship to exist between the Ca number and the ratio of the kinematic viscosities of both phases, $R_{kin} = (\mu_{slag}/\rho_{slag})/(\mu_{steel}/\rho_{steel})$. On this basis, the authors cited above have determined the region of interface instability, where there is a possibility of oil entrapment and the stable interface region, in which no entrapment occurs. Taking the kinematic viscosity values (which were used in the numerical simulations), it has been established that the ratio $R_{kin} = 154$. The limiting value of the Ca number corresponding to this ratio, as determined by the authors of [27], is about $Ca \approx 0.003$. According to these authors, only the phase instability region exists below this value. So, the slag entrapment found in the numerical simulations has been indirectly confirmed by laboratory tests [27].

7. Summary

The examination of the behaviour of the mould powder-originating liquid slag in the mould during continuous steel casting is conducted using laboratory techniques (in water–oil systems), numerical simulations and direct measurement performed under industrial conditions. Their aim is to explain the mechanisms of slag entrapment and to reduce this phenomenon during steel casting.

Numerical simulations require the use of complex mathematical models including appropriate numerical procedures, adequate for the correct determination of the interface in the conditions of interaction of at least three phases. The present study has verified a number of numerical methods, while taking for computation an object constituting a fragment of an immersible pouring tube slab casting mould. The results have demonstrated that when using the VOF method for interface discretization, the First – Order Upwind (Implicit) and Second Order Upwind (Implicit) procedures should not be used, even for a very dense grid. The remaining computational procedures (as listed in Table 2) have exhibited good suitability for such computations. The obtained interfaces of the steel–slag–air system are clear-cut and enable one to assess the degree of liquid slag entrapment into steel due to the occurrence of an instability of shearing stresses at the interface, as explained by the Kelvin - Helmholtz theory. The numerical simulations did not find the formation of von Karman vortices, which could also be the cause of slag entrapment. The absence of von Karman vortices can be explained by the fact that the test mould was regarded as a strictly symmetrical system. The application of the time discretization procedure following the Explicit scheme makes the computation time considerably longer than in the case of using the Implicit scheme - does not have Courant number limitation – can be run with large time steps. The Geo-Reconstruct + Level Set (Explicit) procedure requires a greater time expenditure compared to all of the remaining procedures (for the computation of 2 s of the examined process, an Intel Core i7, 2600CPU, 3.4 GHz computer required 8 hours of computation).

Nomenclature

Ca – Capillary number
Co – Courant number
F_σ – surface tension force
n – vector normal at the interface
Re – Reynolds number
t – time
u – fluid flow velocity
We – Weber number
α_1, α_2, α_k – volume fraction of phase 1, 2, k
Δt – time step of the calculations
Δx – internal length of computational cell
κ – curvature of the interface
μ_1, μ_2, μmix – dinamic viscosity of phase 1, 2 and mixture
ρ_1, ρ_2, ρmix – density of phase 1, 2 and mixture
σ – surface tension
Φ – Level Set function

REFERENCES

[1] L.C. Hibbler, R. Liu, B.G. Thomas, Review of Mould Flux Entrainment Mechanisms and Model Investigation of Entrainment by Shear-Layer Instability, Proceedings 7th ECCC Conference, Dusseldorf (2011).

[2] M. Iguchi, J. Yoshida, T. Shimizu, Y. Mizuno, Model Study on the Entrapment of Mold Powder into Molten Steel, ISIJ International **40**, 685-691 (2000).

[3] N. Kasai, M.Iguchi, Water-model Experiment on Melting Powder Trapping by Vortex in the Continuous Casting Mold **47**, 982-987 (2007).

[4] A. Vakhrushev, M. Wu, A. Ludwig, G. Nitzl, Y. Tang, Gernot Hackl, Experimental Verification of a 3-Phase Continuous Casting Simulation Using a Water Model, Proceedings 8th ECCC Conference, Graz (2014).

[5] K. Tsutsumi, K. Watanabe, M. Suzuki, M. Nakada, Effect of properties of mold powder entrapped in molten steel in a continuous casting process, The South African Institute of Mining and Metallurgy, 803-806 (2004).

[6] Y.S. Gutierrez-Montiel, R.D.Morales, Control of Meniscus Stability in Medium Thickness-straight Walls Slab Mould, ISIJ International **53**, 230-239 (2013).

[7] P. Mishra, S.K. Ajmani, A. Kumar, K.K. Shrivastava, Review article on physical and numerical modelling of SEN and mould for continuous slab casting, International Journal of Engineering Science and Technology (IJEST) **4**, 2234-2243 (2012).

[8] Z. Liu, M. Jiang, F. Tsukihashi, Euler-Euler-Lagrangian Modeling for Two-Phase Flow and Particle Transport in Continuous Casting Mold, ISIJ International **54**, 1314-1323 (2014).

[9] GB.G. Thomas, Q. Yuan, S. Mahmood, R. Liu, R. Chaudhary, Transport and Entrapment of Particles in Steel Continuous Casting, Metallurgical and Materials Transactions B **45B**, 22-35 (2014).

[10] Z. Liu, L. Li, F. Qi, B. Li, M. Jiang, F. Tsukihashi: Population Balance Modeling of Polydispersed Bubbly Flow in Continuous-Casting Using Multiple-Size-Group Approach, Metallurgical and Materials Transactions B **46B**, 406-420 (2014).

[11] P.E. Ramirez-Lopez, P.D. Lee, K.C. Mills, Explicit Modelling of Slag Infiltration and Shell Formation during Mould Oscillation in Continuous Casting, ISIJ International **50**, 425-434 (2010).

[12] I.C. Ramos, R.D. Morales, S. Garcia-Hernandez, Effects of Immersion Depth on Flow Turbulence of Liquid Steel in Slab Mold Using a Nozzle with Upward Angle Rectangular Ports, ISIJ International **54**, 1797-1806 (2014).

[13] A. Jonayat, B.G. Thomas, Transient Thermo-fluid Model of Meniscus Behavior and Slag Consumption in Steel Continuous Casting, Metallurgical and Materials Transactions B **45B**, 1842-1864 (2014).

[14] M. Bielnicki, J. Jowsa, A. Cwudziński, Multiphase numerical model of molten steel and slag behavior in the continuous casting mould, Archives of Metallurgy and Materials **60**, 257-262 (2015).

[15] C.W. Hirt, B.D. Nichols, Volume of Fluid (VOF) Method for the Dynamics of Free Boundaries, Journal of Computational Physics **39**, 201-225 (1981).

[16] V.V. Ranad,: Computational Flow Modeling for Chemical Reactor Engineering, Academic Press, New York (2002).

[17] W.F. Noh, P.R. Woodward, SLICK (Simple Line Interface Calculation, Lecture Notes in Physics **59**, 330-360, (1976).

[18] D.L. Youngs, Time-dependent multi-material flow with large fluid distortion, Numerical Methods for Fluid Dynamics 273-285 (1982).

[19] O. Ubbink, R.I. Issa, Method for capturing sharp fluid interfaces on arbitrary meshes, J. Comput. Phys. **153**, 26-50 (1999).

[20] S. Muzaferija, M. Peric, P. Sames, T. Schelin, A two-fluid Navier-Stokes solver to simulate water entry, Proc. Twenty-Second Symposium on Naval Hydrodynamics (1988).

[21] E. Olsson, G. Kreiss, A conservative Level Set method for two phase flow, J. Comput. Phys. **210**, 225-246 (2005).

[22] O. Ubbink, Numerical prediction of two fluid systems with sharp interfaces, Thesis Ph.D., Imperial College London (1997).

[23] User`s Guide Ansys Fluent, Release 16 (2014).

[24] J.U. Brackbill, D.B. Kothe, C. Zemach, A continuum method for modeling surface tension, J. Comput. Phys. **100**, 335-354 (1992).

[25] S.O Unverdi, G.Tryggvason, A front–tracking method for viscous, incompressible, multi-fluid flow, J. Comput. Phys. **100**, 25-37 (1992).

[26] P.R. Scheller, R. Hagemann, Model investigations on slag entrainment in continuous casting, Archives of Metallurgy and Materials **57**, 283-289 (2012).

[27] R. Hagemann, R. Shwarze, H.P. Heller, P. Scheller, Model Investigation on the Steel-Slag Interface in Continuous-Casting Process, Metallurgical and Materials Transactions B **44B**, 80-90 (2013).

Received: 20 October 2014.